Joint Single-Shot AoD/AoA Estimation in mmW Systems and Analysis under Hardware Impairments

Veljko Boljanovic and Danijela Cabric
Electrical and Computer Engineering Department, University of California, Los Angeles, CA, USA
Email: vboljanovic@ucla.edu, danijela@ee.ucla.edu

Abstract—In millimeter-wave (mmW) networks, beam training enables the base station and user to estimate the dominant angle of departure (AoD) and angle of arrival (AoA) and align their directional beams. With conventional phased arrays, the training requires an exhaustive beam sweeping (EBS), which imposes a large overhead. Alternative array architectures, including digital and true-time-delay arrays, enable simultaneous probing of different angular directions using different frequency components of the signal, which can speed up the training. In this work, we propose a beam training procedure based on frequency-dependent angle probing that uses a single Orthogonal Frequency-Division Multiplexing (OFDM) symbol to jointly estimate the AoD and AoA. We describe the design of the required training codebooks and frequency-domain power-based algorithm. Further, assuming an error-free array at the base station, we analyze how practical hardware impairments in the user's array affect the receive beamforming gain and misalignment probability in beam training. The proposed beam training is evaluated in realistic mmW channels and compared with existing beam training approaches in terms of the misalignment probability, angle estimation accuracy, required overhead, and computational complexity. The results indicate that the proposed algorithm requires a single OFDM symbol and low complexity to achieve a performance comparable to that of the EBS with arrays based on phase shifters.

I. Introduction

In mmW systems, the base station (BS) and user equipment (UE) need to perform beam training to estimate the dominant AoD and AoA and align their steering/combining beams [1]. Early works on mmW beam training considered different variations of the EBS [2], [3], where the BS and UE sequentially check all possible beam pairs to identify the one with the highest received signal power. However, with large antenna arrays and narrow beams at the BS and UE, the beam training overhead in the EBS scales linearly with the number of antennas. In an effort to reduce the training overhead and computational complexity, previous work has explored different digital signal processing (DSP) techniques and array architectures for mmW beam training.

Majority of proposed DSP techniques exploited the sparsity of mmW channels and treated beam training as a compressive sensing problem [4], [5]. It has been shown that the overhead of the compressive algorithms scales logarithmically with the number of antennas [5]. Previous work also considered different array architectures for mmW beam training, including fully digital antenna arrays [6], [7] and hybrid analog-digital arrays [8], [9]. The presence of multiple radio frequency (RF) chains in digital and hybrid arrays allow probing of multiple beams simultaneously, at the cost of a higher power consumption. Further, they can leverage DSP to design beam training codebooks with adaptive sector beams for hierarchical AoD and AoA estimation for a lower training overhead.

The idea of a fast beam training using frequency-dependent beams synthesized by leaky wave antennas [10] or true-time-delay (TTD) arrays [11], [12] was recently proposed and studied analytically and experimentally. By mapping different frequency components of the signal into different directions, both leaky wave antennas and TTD arrays can probe all angular directions in a single shot (training symbol) and extract information of the dominant angle using simple frequency-domain DSP. However, the algorithm design in previous work was limited to UE-only beam training in downlink, i.e., AoA estimation. Further, previous works evaluated the impact of hardware impairments on beam training numerically, but it failed to provide a more analytical explanation on how the gain, phase, and delay errors affect the beam training performance.

In this work, we address the shortcomings of the previous work by designing a beam training algorithm for a joint AoD/AoA estimation using a single OFDM symbol in Sec. III. Then in Sec. IV, we analyze how practical hardware impairments in the UE's array affect the beamforming (BF) gain and misalignment probability in the designed single-shot algorithm. Lastly, in Sec. V, we highlight the advantages of the proposed algorithm over some existing approaches by comparing their performances in realistic mmW channels.

II. System Model

We consider downlink beam training between the BS and UE using only one OFDM symbol. The carrier frequency, bandwidth, and number of subcarriers are denoted as f_c, BW, and M_{tot}, respectively. The OFDM symbol uses M ($M \leq M_{tot}$) subcarriers from the predefined set $\mathbb{M}$, all loaded with binary phase shift keying (BPSK) modulated pilots. We assume that the BS is equipped with a fully digital antenna array [13] that does not have hardware impairments. The UE is assumed to have a fully connected hybrid TTD array affected by hardware impairments. Similar to the sub-array architecture in [11], the hybrid array has N_{RF} RF RF chains and a delay element in each antenna branch.

This work was supported by NSF under grant 1955672.

In this work, we consider a frequency-selective mmW channel with L multipath clusters. The channel matrix $\mathbf{H}[m] \in \mathbb{C}^{N_R \times N_T}$ at the m-th subcarrier is defined as

$$\mathbf{H}[m] = \sum_{l=1}^{L} g_l[m]\mathbf{a}_R(\theta_l^{(R)})\mathbf{a}_T^H(\theta_l^{(T)}), \quad (1)$$

where $g_l[m] \sim \mathcal{CN}(0, \sigma_N^2)$, $\theta_l^{(T)}$, and $\theta_l^{(R)}$ are a complex gain, AoD, AoA of the l-th cluster, respectively. The gains $g_l[m]$, $\forall l, m$, are assumed to be independent across L multipath clusters and non-neighboring subcarriers.

Let $\mathbf{v}[m] \in \mathbb{C}^{N_T}$ be the BS digital precoder for the m-th subcarrier. Given (1), the received signal $y_r[m]$ at the m-th subcarrier in the r-th RF chain can be expressed as

$$y_r[m] = \mathbf{w}_r^H[m]\mathbf{H}[m]\mathbf{v}[m]s[m] + \mathbf{w}_r^H[m]\mathbf{n}[m], \ m \in \mathcal{M}, \quad (2)$$

where $\mathbf{w}_r[m] \in \mathbb{C}^{N_R}$ is the UE analog TTD combiner for the m-th subcarrier in the r-th RF chain, $s[m]$ is a BPSK pilot at the m-th subcarrier, and $\mathbf{n}[m] \sim \mathcal{CN}\left(\mathbf{0}, \sigma^2 \mathbf{I}_{N_R}\right)$ is white Gaussian noise. The UE combiners $\mathbf{w}_r[m]$, $\forall r, m$, are assumed to be affected by time-invariant gain, delay, and phase errors. We model hardware impairments as Gaussian random variables [14]. In the n-th antenna branch, we model the distorted gain as a Gaussian random variable in log-scale, i.e., $10\log_{10}(\tilde{\alpha}_n) \sim \mathcal{N}\left(0, \sigma_A^2\right)$, or equivalently as a lognormal random variable with the base 10 in linear scale, i.e., $\tilde{\alpha}_n \sim \text{Lognormal}_{10}\left(0, \sigma_A^2/100\right)$. The distorted delay tap is modeled as $\tilde{\tau}_n = \tau_n + \tilde{\tau}_n$, where τ_n is a desired delay tap and $\tilde{\tau}_n \sim \mathcal{N}\left(0, \sigma_n^2\right)$ is a random delay error. Similarly, in the r-th RF chain, the distorted phase tap is modeled as $\tilde{\varphi}_{r,n} = \varphi_{r,n} + \varphi_{r,n}$, where $\varphi_{r,n}$ is a desired phase tap and $\varphi_{r,n} \sim \mathcal{N}\left(0, \sigma_P^2\right)$ is a random phase error. With the described hardware impairments, the n-th element of $\mathbf{w}_r[m]$ is

$$[\mathbf{w}_r[m]]_n = \tilde{\alpha}_n \exp\left(-j\left(2\pi(f_m - f_c)\tilde{\tau}_n + \varphi_{r,n}\right)\right), \quad (3)$$

where f_m is the frequency of the m-th subcarrier, defined as $f_m = f_c - BW/2 + (m-1)BW/(M_{tot}-1)$.

III. Single-Symbol Beam Training Algorithm

In this section, we describe the design of frequency-dependent codebooks and DSP algorithm which requires only one OFDM symbol for a joint AoA and AoA estimation in frequency-selective mmW channels.

A. Design of Beam Training Codebooks

Unlike in the UE-only beam training in [11], joint AoD and AoA estimation requires frequency-dependent codebooks to be designed both at the BS and UE side. There are $N_T N_R$ beam pairs that need to be considered in the training. The key codebook design idea is to map OFDM subcarriers into different beam pairs. Thus, the set of used subcarriers $\mathcal{M}$ has $M = N_T N_R$ elements. The total of M_{tot} subcarriers is divided into N_R groups, and in each group, the first N_T subcarriers are selected and loaded with BPSK pilots. Mathematically, the set $\mathcal{M}$ is defined as $\mathcal{M} = \{m \mid m = m_T + (m_R - 1)\lfloor M_{tot}/(N_R)\rfloor, m_T = 1, \cdots, N_T, m_R = 1, \cdots, N_R\}$, where $\lfloor x \rfloor$ rounds x to the nearest lower integer. At the BS side, we design a codebook where in each of the N_R groups, the N_T subcarriers are assigned N_T different discrete Fourier transform (DFT) precoders $\mathbf{u}_{m_T}$, $m_T = 1, \ldots, N_T$, that cover the entire angular range $(-\pi/2, \pi/2)$. Equivalently, the subcarriers from the set $\mathcal{M}_{m_T}^{(T)} = \{m \mid m = m_T + (m_R - 1)\lfloor M_{tot}/(N_R)\rfloor, m_R = 1, \ldots, N_R\}$ are assigned the m_T-th DFT precoder, i.e, $\mathbf{v}[m] = \mathbf{u}_{m_T}$, $m \in \mathcal{M}_{m_T}^{(T)}$. At the UE side, we focus on the first RF chain and design a codebook where the N_T subcarriers from the set $\mathcal{M}_{m_R}^{(R)} = \{m \mid m = m_T + (m_R - 1)\lfloor M_{tot}/(N_R)\rfloor, m_T = 1, \ldots, N_T\}$ are assigned the same DFT combiner $\mathbf{f}_{m_R}$, i.e., $\mathbf{w}_1[m] = \mathbf{f}_{m_R}$, $m \in \mathcal{M}_{m_R}^{(R)}$. The design of training codebooks is illustrated on a small example in Fig. 1.

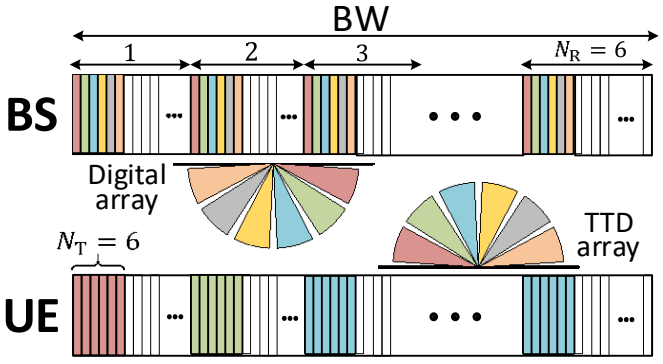

Fig. 1. Illustration of subcarrier selection and codebook design at the BS and UE, assuming $N_T = 6$ and $N_R = 6$.

Since the BS is equipped with a digital array, its codebook can be easily designed through the frequency-domain DSP by precoding N_T samples at each used subcarrier with its corresponding DFT beam. On the other hand, the UE codebook is created by setting the delay taps τ_n, $\forall n$, and phase taps $\varphi_{r,n}$, $\forall r, n$. We set the delay taps as follows

$$\tau_n = (n-1)/BW, \ 1 \le n \le N_R, \quad (4)$$

to probe all AoAs in the range $(-\pi/2, \pi/2)$. The N subcarriers from the set $\mathcal{M}_1^{(R)}$ correspond to different frequencies and thus they experience slightly different combining angles and beamforming gains. The difference in beamforming gains is reduced by using the phase shifters to align the UE codebook. The alignment phase tap is the same in all RF chains and for the n-th antenna it is given as

$$\varphi_{al,n} = -(n-1)\text{mod}\left(2\pi(f_{mid} - f_c)/BW + \pi, 2\pi\right), \quad (5)$$

where $f_{mid} = f_{N_T/2} + BW/(2M_{tot} - 2)$ is the "middle" frequency of the subcarriers in $\mathcal{M}_1^{(R)}$ and mod() is the modulo operator. To increase the robustness to frequency-selective channels through frequency diversity, we rotate the UE codebook in different RF chains by using the rotation phase taps

$$\varphi_{rot,r,n} = (r-1)(n-1)2\lfloor N_R/N_{RF}\rfloor\pi/N_R, \ \forall r, n. \quad (6)$$

These taps ensure that the codebook diversity is $R = N_{RF}$, i.e., that each AoD-AoA beam pair is probed by N_{RF} different subcarriers in different RF chains. Thus, the overall phase taps are set as follows

$$\varphi_{r,n} = \varphi_{al,n} + \varphi_{rot,r,n}, \quad 1 \le r \le N_{RF}, 1 \le n \le N_R. \tag{7}$$

The designed codebooks experience two main challenges. First, the maximum number of beam pairs that can be probed is limited by the total number of subcarriers M_{tot}. Thus, with large antenna arrays and $M = N_T N_R > M_{tot}$, the proposed beam training requires a different implementation with more than one OFDM symbol. Second, the total received signal power in the proposed beam training with frequency-dependent beams is roughly $M/(N_{RF}L)$ times smaller than that in the conventional EBS. For this reason, the proposed beam training requires either a higher transmit power at the BS or a smaller distance between the BS and UE than the EBS.

B. DSP Algorithm for Beam Training

We use the designed BS and UE beam training codebooks to develop a DSP algorithm for joint AoD and AoA estimation. We propose a non-coherent power-based algorithm that does not rely on phase information in samples in (2). Non-coherent approaches have often been considered in previous work and practical implementations due to their robustness to phase noise and frequency offset. The proposed algorithm in this paper resembles the ones in [11], but it accounts for the dependency of the UE BF gains on hardware impairments.

The channel matrix at the m-th subcarrier in (1) can be considered as a frequency-domain realization of the matrix $H = \sum_{l=1}^{L} g_l a_R(\theta_l^{(R)}) a_T^H(\theta_l^{(T)})$ [11]. Channel realizations that correspond to non-neighboring subcarriers are independent.

Let b be the index of the beam pair defined by the precoder u_{m_T} and combiner f_{m_R}. We define the set of $R = N_{RF}$ subcarriers that probe the b-th beam pair as $M_b^{(B)} = \{m | m = \text{mod}(m_b + (r-1)\lfloor \frac{N_R}{N_{RF}} \rfloor \lfloor \frac{M_{tot}}{N_R} \rfloor, M), r = 1, \ldots, R\}$. The R non-neighboring subcarriers from $M_b^{(B)}$ experience different channels, which allows us to consider the channel matrices $H[m]$, $m \in M_b^{(B)}$, as independent realizations of the matrix $H = \sum_{l=1}^{L} g_l a_R(\theta_l^{(R)}) a_T^H(\theta_l^{(T)})$ [11]. Similarly, the received samples $Y[m]$, $m \in M_b^{(B)}$, are independent realizations of $y_b = f_{m_R}^H H u_{m_T} s + f_{m_R}^H n$. Then the expected received power for the b-th beam pair is given as $p_b = E[|y_b|^2] = E[(f_{m_R}^H H u_{m_T} s + f_{m_R}^H n)^H (f_{m_R}^H H u_{m_T} s + f_{m_R}^H n)]$. Assuming $|s|^2 = 1/M$ and the independence between the channel gains and thermal noise, we can use the derivation in [11] to express p_b, $\forall b$, as $p_b = \sum_{l=1}^{L} g_l^2 |a_T^H(\theta_l^{(T)}) u_{m_T}|^2 E\left[|f_{m_R}^H a_R(\theta_l^{(R)})|^2\right] + E\left[|f_{m_R}^H n|^2\right]$. Unlike in [11], the p_b in this work considers frequency-dependent UE BF gains $|f_{m_R}^H a_R(\theta_l^{(R)})|^2$, $\forall l$. Namely, the R combiners $w_r[m]$, $\forall r, m \in M_b^{(B)}$, aligned with f_{m_R}, are differently affected by hardware impairments, which leads to different BF gains. This happens for two reasons: 1) the phase errors $\tilde{\varphi}_{r,n}$, $\forall r, n$, are independent across all antenna elements and RF chains that synthesize the combiners; 2) the delay errors $\tilde{\tau}_n$, $\forall n$, have different impact on the subcarriers $m \in M_b^{(B)}$. Therefore, the expected power can be rewritten to include the average BF gain across the R RF chains and subcarriers from $M_b^{(B)}$, as follows

$$p_b = \sum_{l=1}^{L} \frac{\sigma_l^2}{M} |a_T^H(\theta_l^{(T)}) u_{m_T}|^2 \sum_{r,m \in M_b^{(B)}} \frac{|w_r^H[m] a_R(\theta(R^{(l)}))|^2 l=1}{R} + \sum_{r,m \in M_b^{(B)}} \frac{|w_r^H[m] n[m]|^2}{R}. \tag{8}$$

Given the samples $y_r[m]$, $\forall r, m$, of one OFDM symbol, the expected beam pair power p_b, is estimated by averaging out the powers at the subcarriers from $M_b^{(B)}$ from their corresponding RF chains $r = 1, \ldots, R$:

$$\hat{p}_b = \frac{1}{R} \sum_{r,m \in M_b^{(B)}} |y_r[m]|^2. \tag{9}$$

The AoD and AoA estimates are based on the beam pair index $\hat{b}$ that corresponds to the maximum measured power $\hat{p}_{max} = \max_{\hat{p}_b} \hat{p}_b$. Let $\xi_{m_T^{\hat{}}}^{(T)}$ and $\xi_{m_R^{\hat{}}}^{(R)}$ be the steering angles that correspond to $\hat{b}$ at the BS and UE side, respectively. Then the on-grid AoD and AoA estimates are

$$\theta^{(T)} = \xi_{m_T^{\hat{}}}^{(T)}, \quad \theta^{(R)} = \xi_{m_R^{\hat{}}}^{(R)} \tag{10}$$

The expected power p_b in (8) is affected by hardware impairments through the UE BF gains $|w_r^H[m] a_R(\theta_l(R^{(l)}))|^2$, $\forall r, m \in M_b^{(B)}, \forall l$, and power of post-combining noise $|w_r^H[m] n[m]|^2$, $\forall r, m \in M_b^{(B)}$. In the next section, we derive the statistics of p_b with respect to hardware impairments and then leverage them to analyze the beam pair misalignment probability in mmW channels.

IV. Impact of Hardware Impairments

In this section we derive the statistics of p_b, $\forall b$, including the mean values μ_b, $\forall b$, and variances β_b, $\forall b$, with respect to random hardware impairments and then use them to analyze the beam pair misalignment probability.

For mathematical tractability, we assume that the UE BF gains and post-combining noise powers are uncorrelated in different RF chains. Then the mean μ_b can be expressed as

$$\mu_b = \sum_{l=1}^{L} C_l \sum_{r,m \in M_b^{(B)}} \frac{E\left[G_{r,m,l}^{(R)}\right]}{R} + \sum_{r,m \in M_b^{(B)}} \frac{E[N_{r,m}]}{R}, \tag{11}$$

where $C_l = \sigma_l^2 |a_T^H(\theta_l^{(T)}) u_{m_T}|^2 / M$, $N_{r,m} = |w_r^H[m] n[m]|^2$, and $G_{r,m,l}^{(R)} = |w_r^H[m] a_R(\theta_l(R^{(l)}))|^2$. Similarly, the variance β_b can be expressed as

$$\beta_b = \sum_{l=1}^{L} C_l^2 \sum_{r,m \in M_b^{(B)}} \frac{Var\left[G_{r,m,l}^{(R)}\right]}{R^2} + \sum_{r,m \in M_b^{(B)}} \frac{Var[N_{r,m}]}{R^2}. \tag{12}$$

The expressions (11) and (12) indicate that μ_b, $\forall b$, and β_b, $\forall b$, depend on the statistics of the UE BF gains $G^{(R)}_{r,m,l}$, $\forall r,m,l$, and post-combining noise power $N_{r,m}$, $\forall r,m$, which we derive in the following subsection.

A. Statistics of BF Gains and Post-Combining Noise Power

The inner product $w^H_r[m]a_R(\theta^{(R)}_l)$ is defined as $w^H_r[m]a_R(\theta^{(R)}_l) = \frac{1}{\sqrt{N_R}} \sum_{n=1}^{N_R} \bar{\alpha}_n e^{j\bar{\psi}_{r,n}}$, where $\bar{\psi}_{r,n} = \psi_{r,n} + \tilde{\psi}_{r,n}$ with $\psi_{r,n} = 2\pi(f_m - f_c)\tau_n + \varphi_{r,n} - (n-1)\pi\sin(\theta^{(R)}_l)$ being the deterministic value and $\tilde{\psi}_{r,n} = 2\pi(f_m - f_c)\tilde{\tau}_n + \tilde{\varphi}_n$ being a Gaussian random variable with distribution $\mathcal{N}(0, \sigma^2_\psi)$. Since the delay and phase errors are independent, the variance σ^2 is equal to $\sigma^2 = 4\pi^2(f_m - f_c)^2\sigma^2_\tau + \sigma^2_\varphi$. Thus, $\psi_{r,n}$ is a Gaussian random variable with distribution $\psi_{r,n} \sim \mathcal{N}(\psi_{r,n}, \sigma^2_\psi)$. Using the expression for the inner product and Euler's formula, the BF gain is calculated as

$$G^{(R)}_{r,m,l} = \frac{1}{N_R} \sum_{n_1=1}^{N_R} \sum_{n_2=1}^{N_R} \bar{X}_{r,n_1,n_2}, \tag{13}$$

where $\bar{X}_{r,n_1,n_2} = I_{r,n_1} I_{r,n_2} + Q_{r,n_1} Q_{r,n_2}$, $I_{r,n} = \bar{\alpha}_n \cos(\bar{\psi}_{r,n})$, and $Q_{r,n} = \bar{\alpha}_n \sin(\bar{\psi}_{r,n})$. The calculation of the mean value $\mathbb{E}\left[G^{(R)}_{r,m,l}\right]$ and variance $\mathrm{Var}\left[G^{(R)}_{r,m,l}\right]$ require the knowledge of lower and higher order moments of $\bar{\alpha}_n, \forall n$, $I_{r,n}, \forall r,n$, and $Q_{r,n}, \forall r,n$. These moments can be derived using the properties of a complex exponential transformation $e^{j\bar{\psi}_{r,n}}$, as summarized in the Appendix.

The calculation of $\mathbb{E}\left[G^{(R)}_{r,m,l}\right]$ includes two distinct cases for the indices n_1 and n_2: 1) $n_1 = n_2$; 2) $n_1 \neq n_2$. When $n_1 = n_2$, the mean value is

$$\mathbb{E}\left[\bar{X}_{r,n_1,n_1}\right] = \mathbb{E}\left[I^2_{r,n_1}\right] + \mathbb{E}\left[Q^2_{r,n_1}\right] = 2e^{\frac{(\ln(10))^2\sigma^2_A}{50}}. \tag{14}$$

On the other hand, when $n_1 \neq n_2$, the mean value is

$$\mathbb{E}\left[\bar{X}_{r,n_1,n_2}\right] = e^{\frac{(\ln(10))^2\sigma^2_A}{100} - \sigma^2_\psi}\cos(\psi_{r,n_1} - \psi_{r,n_2}). \tag{15}$$

If we denote $\Delta\psi_r = 2\pi(f_m - f_c)\Delta\tau + \Delta\varphi_r - \pi\sin(\theta^{(R)}_l)$, the expression in (15) can be further simplified in the following way

$$\mathbb{E}\left[\bar{X}_{r,n_1,n_2}\right] = e^{\frac{(\ln(10))^2\sigma^2_A}{100} - \sigma^2_\psi}\cos((n_1 - n_2)\Delta\psi_r). \tag{16}$$

Finally, by introducing $n' = n_1 - n_2$ and using the results for the two cases, the mean BF gain $\mathbb{E}\left[G^{(R)}_{r,m,l}\right]$ can be calculated as follows

$$\mathbb{E}\left[G^{(R)}_{r,m,l}\right] = e^{\frac{(\ln(10))^2}{50}\sigma^2_A} + e^{\frac{(\ln(10))^2}{100}\sigma^2_A - 4\pi^2(f_m - f_c)^2\sigma^2_\tau - \sigma^2_\varphi} \times 2\sum_{n'} (N_R - n')\cos(n'\Delta\psi_r)/N_R \tag{17}$$

The variance $\mathrm{Var}\left[G^{(R)}_{r,m,l}\right]$ is calculated as $\mathrm{Var}\left[G^{(R)}_{r,m,l}\right] = \mathbb{E}\left[G^{(R)}_{r,m,l}{}^2\right] - \mathbb{E}\left[G^{(R)}_{r,m,l}\right]^2$. The second moment $\mathbb{E}\left[G^{(R)}_{r,m,l}{}^2\right]$ can be calculated using the derived higher order moments of $\bar{\alpha}_n, \forall n$, $I_{r,n}, \forall r,n$, and $Q_{r,n}, \forall r,n$, from the Appendix. Thus, using the second moment and the result in (17), we can determine the UE BF gain variance.

The post-combining noise power $N_{r,m}$ is defined as

$$N_{r,m} = \sum_{n_1=1}^{N_R} \sum_{n_2=1}^{N_R} \tilde{Z}_{r,n_1,n_2}, \tag{18}$$

where $\tilde{Z}_{r,n_1,n_2} = [w^*_r[m]]_{n_1}[n^*[m]]_{n_1}[w_r[m]]_{n_2}[n[m]]_{n_2}$. Based on the independence between hardware impairments and thermal noise, the mean is $\mathbb{E}\left[\tilde{Z}_{r,n_1,n_2}\right] = \mathbb{E}\left[w^*_r[m]]_{n_1}[w_r[m]]_{n_2}\right]\mathbb{E}\left[[n^*[m]]_{n_1}[n[m]]_{n_2}\right]$. Further, from the independence among the elements of $n[m]$, it follows that $\mathbb{E}\left[[n^*[m]]_{n_1}[n[m]]_{n_2}\right] = \mathbb{E}\left[|[n[m]]_{n_1}|^2\right]$ for $n_1 = n_2$ and $\mathbb{E}\left[[n^*[m]]_{n_1}[n[m]]_{n_2}\right] = 0$ for $n_1 \neq n_2$. It can be shown that $|[n[m]]_{n_1}|^2$ is exponentially distributed with the mean value $\mathbb{E}\left[|[n[m]]_{n_1}|^2\right] = 2\sigma^2$. Thus, we can express the mean value $\mathbb{E}[N_{r,m}]$ of the post-combining noise power as

$$\mathbb{E}[N_{r,m}] = \sum_{n=1}^{N_R} \mathbb{E}\left[\bar{\alpha}^2_n\right]\mathbb{E}\left[|[n[m]]_n|^2\right] = 2N_R\sigma^2 e^{\frac{(\ln(10))^2\sigma^2_A}{50}}, \tag{19}$$

Similarly as for the BF gains, the variance $\mathrm{Var}[N_{r,m}]$ is defined as $\mathrm{Var}[N_{r,m}] = \mathbb{E}\left[N^2_{r,m}\right] - (\mathbb{E}[N_{r,m}])^2$. It can be shown that the second moment is

$$\mathbb{E}\left[N^2_{r,m}\right] = 8N_R\sigma^4_N e^{\frac{(\ln(10))^2\sigma^2_A}{12.5}} + (N_R - 1)e^{\frac{(\ln(10))^2\sigma^2_A}{25}}. \tag{20}$$

Thus using the expressions for the second moment in (20) and mean value in (19), we can calculate the variance $\mathrm{Var}[N_{r,m}]$.

B. Beam Pair Misalignment Probability

Let p_o and p_{no} be the expected powers that correspond to the optimal beam pair aligned with the dominant AoD and AoA and non-optimal beam pair with the highest power, respectively. Mathematically, the power p_{no} is defined as $p_{no} = \max_{p_b, p_b \neq p_o} p_b$. Our goal is to evaluate the probabil-ity $P[p_o < p_{no}]$, which requires knowledge of the probability density functions (PDF)s of p_o and p_{no}, i.e., knowledge of the PDFs of $p_b, \forall b$ in (8). Finding the exact PDFs is a complex task, and thus, for mathematical tractability, we assume that the expected powers $p_b, \forall b$, follow Gumbel$(\lambda_b, \delta_b), \forall b$, distributions, where $\delta_b = \sqrt{6\beta_b/\pi^2}, \forall b$, and $\lambda_b = \mu_b - 0.5772\delta_b, \forall b$. It can be demonstrated numerically that the assumed Gumbel distributions represent a good fit for simulated PDFs of $p_b, \forall b$. The mean μ_o and variance β_o associated with the optimal beam pair are directly used to calculate the parameters of $p_o \sim$ Gumbel(λ_o, δ_o), i.e., $\delta_o = \sqrt{6\beta_o/\pi^2}$ and $\lambda_o = \mu_o - 0.5772\delta_o$. On the other hand, the statistics of p_{no} depend on the highest power of the remaining $M-1$ beam pairs. Using the sparsity of mmW channels, we approximate the $M-1$ beam pairs using the $4L-1$ beam pairs with significant power, as illustrated in Fig. 2. The powers of all $4L-1$ Gumbel distributed beam pairs $\{b_i\}_{i=1}^{4L-1}$ are assumed to be independent and have the same

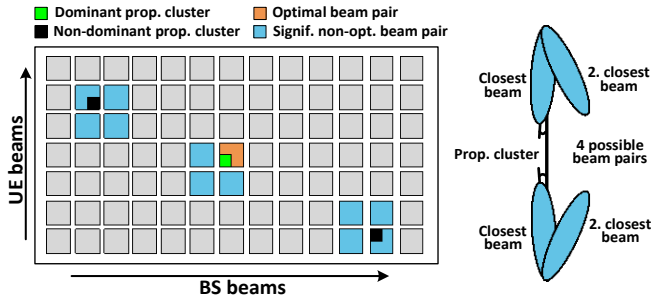

Fig. 2. Illustration of beam pairs with significant power in a channel with three propagation clusters. There are 4 significant beam pairs around each cluster and they include 2 beams at the BS, which are closest to the cluster AoD, and two beams at the UE, which are closest to the cluster AoA, as illustrated on the right-hand side.

scale parameter defined as $\delta = \max_{b_i} \delta_{b_i}$, while the location parameters λ_{b_i}, b_i, can be different. Using the independence of the powers, the cumulative distribution function (CDF) of p_{no} is given as follows

$$P[p_{no} \leq p] = e^{-e^{-\left(p-\delta \ln\left(\sum_{i=1}^{4L-1} e^{\lambda_{b_i}/\delta}\right)\right)/\delta}} \quad (21)$$

From (21), we can conclude that $p_{no} \sim \text{Gumbel}(\lambda_{no}, \delta_{no})$, where $\delta_{no} = \delta$ and $\lambda_{no} = \delta \ln\left(\sum_{i=1}^{4L-1} e^{\lambda_{b_i}/\delta}\right)$. The mean and variance of p_{no} are $\mu_{no} = \lambda_{no} + 0.5772\delta_{no}$ and $\beta_{no} = \pi^2\delta_{no}^2/6$, respectively. Given the Gumbel random variables p_o and p_{no}, we define the difference $p_{diff} = p_o - p_{no}$ and use it to determine the beam pair misalignment probability. When distributions of p_o and p_{no} have the same parameters, which is a low probability event, the difference p_{diff} follows a logistic distribution. In all other cases, p_{diff} can be treated as another Gumbel random variable $p_{diff} \sim \text{Gumbel}(\lambda_{diff}, \delta_{diff})$, where $\delta_{diff} = \sqrt{6\beta_{diff}/\pi^2}$, $\lambda_{diff} = \mu_{no} - 0.5772\delta_{diff}$, $\delta_{diff} = \beta_o + \beta_{no}$, and $\mu_{diff} = \mu_o - \mu_{no}$. Thus, the beam pair misalignment probability is given as follows

$$P[p_{diff} < 0] = e^{-e^{-(p-\lambda_{diff})/\delta_{diff}}}\Big|_{p=-\infty}^{p=0} = e^{-e^{\lambda_{diff}/\delta_{diff}}}. \quad (22)$$

C. Misalignment Probability in Simplified mmW Channels

In this subsection, we numerically evaluate the result in (22) and compare it with simulated curves in the presence of "medium" hardware impairments. We assume $f_c = 28$ GHz, $BW = 2$ GHz, $M_{tot} = 4096$, $N_T = 64$, $N_R = 16$, $M = N_T N_R = 1024$, $R = N_{RF} = \{2, 4, 8\}$, and $(\sigma_A, \sigma_P, \sigma_T) = (0.5\text{ dB}, 45^\circ, 100\text{ ps})$. To get a better understanding of the impact of hardware impairments, we focus on the high signal-to-noise ratio (SNR) case with $\text{SNR} = \sum_{l=1}^{L} \sigma_l^2/\sigma_N^2 = 30$dB and negligible post-combining noise power $N_{r,m}$, r, m. We consider a sparse channel with $L = 3$ multipath clusters. Without loss of generality, we can assume that the first cluster is always dominant and thus determines the optimal beam pair. The angles of the first cluster $\theta_1^{(R)}$ and $\theta_1^{(T)}$ are jointly swept from 0° (0 rad phase) to $\sin^{-1}(1/N_R)$ (π/N_R rad phase) and $\sin^{-1}(1/N_T)$ (π/N_T rad phase), respectively, while the angles of other clusters are generated randomly. In this setup, the optimal beams at the BS and UE are both pointing at 0°. The sweeping of $\theta_1^{(T)}$ and $\theta_1^{(R)}$ allows us to precisely evaluate the misalignment probability in cases when the optimal beam pair is not aligned with the AoD and AoA.

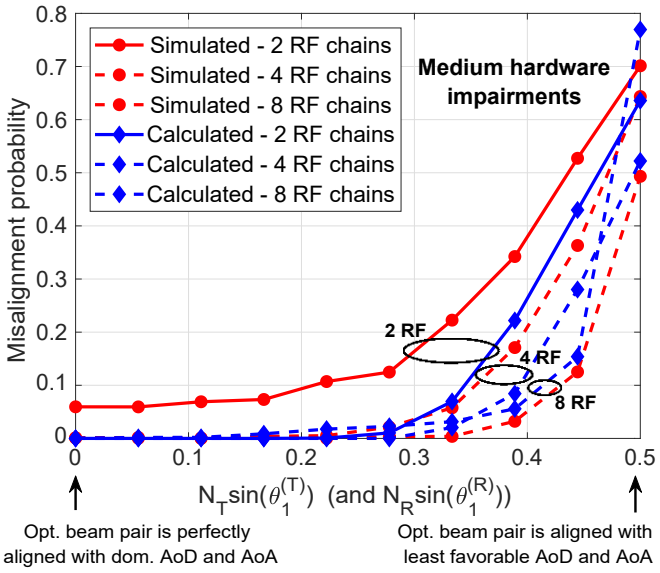

Fig. 3. Calculated versus simulated beam pair misalignment probability in the presence of medium hardware impairments. The x-axis is common for both the BS and UE and it represents the normalized phase associated with the dominant AoD $\theta_1^{(T)}$ and AoA $\theta_1^{(R)}$.

In Fig. 3, we show the results for the calculated and simulated beam pair misalignment probability. The results indicate that the theoretical and simulated curves improve and become more similar as N_{RF} increases. The theoretical curve improves because the variances β_b, b, in (12) become smaller with higher R, which shrinks the distributions of p_o and p_{no} and thus allows a more reliable estimation of the optimal beam pair in the presence of hardware impairments. Similarly, the simulated curve improves because the variance of the sample mean estimator in (9) decreases, i.e., the power estimates become more precise as the channel gains and UE BF gains affected by hardware errors are averaged out across more subcarriers. The misalignment probability increases significantly when the AoD and AoA phases approach the values π/N_T and π/N_R that correspond to the intersections between the optimal and closest non-optimal DFT beams at the BS and UE, respectively.

V. Numerical Results

In this section, we aim to further evaluate the performance of the proposed single-symbol beam training and to compare it with the benchmark approaches based on non-coherent (phase-less) measurements. The benchmark approaches include the EBS and non-coherent compressive sensing (NCS) [5]. In both benchmark approaches, we assume that the UE hybrid array does not have delay elements and it is, therefore, insensitive to

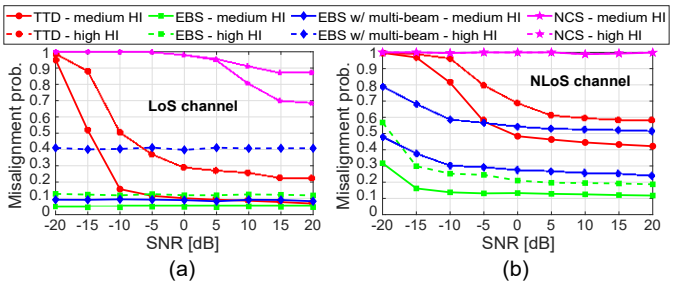

Fig. 4. Comparison in terms of the beam pair misalignment probability between the proposed and benchmark algorithms in realistic (a) LoS and (b) NLoS mmW scenarios.

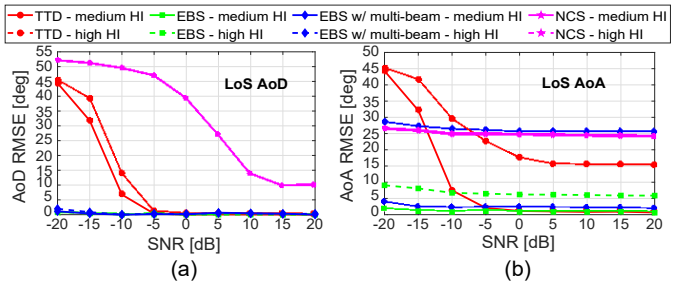

Fig. 5. Comparison in terms of the RMSE of (a) dominant AoD estimation and (b) dominant AoA estimation, between the proposed and benchmark algorithms in LoS mmW channel.

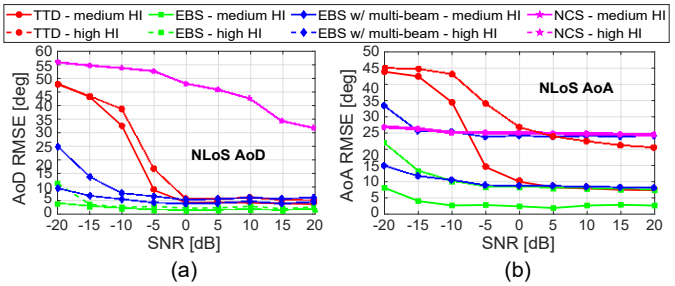

Fig. 6. Comparison in terms of the RMSE of (a) dominant AoD estimation and (b) dominant AoA estimation, between the proposed and benchmark algorithms in NLoS mmW channel.

delay errors. All simulations are performed in realistic line-of-sight (LoS) and non-line-of-sight (NLoS) mmMAGIC channels generated by the Quadriga channel simulator [15]. We assume $R = N_{RF} = 4$, medium hardware impairments with ($\sigma_A = 0.5$ dB, $\sigma_P = 45^\circ$, $\sigma_T = 100$ ps), high hardware impairments with ($\sigma_A = 1$ dB, $\sigma_P = 70^\circ$, $\sigma_T = 150$ ps), and $T_{NCS} = 15$ symbols for AoD/AoA estimation in the NCS.

In Fig. 4, the misalignment probabilities of the proposed and benchmark approaches are compared. With medium hardware impairments, the proposed TTD-based training, EBS, and EBS with multi-beam probing (N_{RF} beams probed simultaneously) achieve a similar performance in medium and high SNRs in LoS channels. However, due to a limited codebook diversity R, the proposed approach results in a higher misalignment probability in NLoS and low-SNR LoS channels than the EBS and EBS with multi-beam probing, which align all used subcarriers in each probed direction and thus use a codebook with "full diversity" ($R = M$). For the same reason, the EBS has a better performance with high hardware impairments than the TTD-based training. However, it is important to note that the proposed TTD-based training was simulated in the presence of gain, phase, and delay errors, while delay errors were not considered in the EBS. Previously, the NCS was shown to work well in single-path channels [5]. However, Fig. 4 indicates that the AoD/AoA estimation with the NCS is less reliable in the presence of hardware impairments in realistic channels.

The proposed beam training approach is also compared with the benchmarks and the results for LoS and NLoS channels are presented in Fig. 5 and Fig. 6, respectively. Similar as for the misalignment probability, the proposed approach achieves a comparable performance as the EBS and EBS with multi-beam probing. A relatively low AoA estimation error in medium hardware impairments suggests that the estimated UE beam is often close to the optimal one. With large hardware errors, however, the AoA estimation accuracy deteriorates for all of the considered beam training approaches.

A. Overhead and Computational Complexity

We also compare the proposed and benchmarks approaches in terms of the required beam training overhead. The conventional EBS requires the highest overhead, which scales as $O(N_R)$. However, N_{RF} RF chains at the UE can be leveraged to probe multiple directions at the same time, which reduces the EBS overhead to $O(N_R/N_{RF})$. Previous work on the NCS showed that the required number of symbols in beam training scales logarithmically with the number of antennas, i.e., $O(\log(N_R))$ [5]. On the other hand, the proposed beam training requires a single OFDM symbol, i.e., $O(1)$.

Lastly, we compare the proposed and benchmarks training approaches in terms of computational complexity. The EBS and EBS with multi beam probing have the highest complexity as they require $O(M^2 N_{RF} + M)$ operations to average out the received signal powers of M beam pairs across M subcarriers in N_{RF} chains and to find the beam pair with the highest received signal power. The NCS needs less operations for averaging, but it introduces additional complexity to calculate the correlation between the power signatures [5]. Its complexity scales as $O(2T_{NCS}(N_T + N_R) + N_R + N_T)$. The proposed TTD-based beam training algorithm has the lowest complexity. Due to the codebooks, the complexity of averaging out the powers and finding the best beam pair scales as $O(M N_{RF} + M)$.

VI. Conclusions

This work introduced and analyzed a single-symbol AoD and AoA estimation that relies on frequency-dependent beam probing at the BS and UE. We demonstrated that with a proper design of training codebooks, a simple power-based DSP algorithm can be designed for a reliable estimation of the best pair of steering directions. Detailed analysis of the impact

TABLE I
SUMMARY OF STATISTICAL MOMENTS

$E[\bar{\alpha}_n]$	$e^{(\ln(10))^2\sigma_A^2/200}$
$Var[\bar{\alpha}_n]$	$e^{(\ln(10))^2\sigma_A^2/100}(e^{(\ln(10))^2\sigma_A^2/100}-1)$
$E[\bar{\alpha}_n^i]$	$e^{i^2(\ln(10))^2\sigma_A^2/200}$
$E[\cos(\psi_{r,n})]$	$e^{-\sigma_\psi^2/2}\cos(\psi_{r,n})$
$E[\sin(\psi_{r,n})]$	$e^{-\sigma_\psi^2/2}\sin(\psi_{r,n})$
$E[\cos(\psi_{r,n})\sin(\psi_{r,n})]$	$e^{-2\sigma_\psi^2}\sin(2\psi_{r,n})/2$
$E[\cos^2(\psi_{r,n})]$	$1/2+e^{-\sigma_\psi^2/2}\cos(2\psi_{r,n})/2$
$E[\sin^2(\psi_{r,n})]$	$1/2-e^{-\sigma_\psi^2/2}\cos(2\psi_{r,n})/2$
$E[\cos^2(\psi_{r,n})\sin(\psi_{r,n})]$	$e^{-9\sigma_\psi^2/2}\sin(3\psi_{r,n})/4-$ $e^{-\sigma_\psi^2/2}\sin(\psi_{r,n})/4$
$E[\cos(\psi_{r,n})\sin^2(\psi_{r,n})]$	$e^{-\sigma_\psi^2/2}\cos(\psi_{r,n})/4-$ $e^{-9\sigma_\psi^2/2}\cos(3\psi_{r,n})/4$
$E[\cos^3(\bar{\psi}_{r,n})]$	$3e^{-\sigma_\psi^2/2}\cos(\psi_{r,n})/4+$ $e^{-9\sigma_\psi^2/2}\cos(3\psi_{r,n})/4$
$E[\sin^3(\bar{\psi}_{r,n})]$	$3e^{-\sigma_\psi^2/2}\sin(\psi_{r,n})/4-$ $e^{-9\sigma_\psi^2/2}\sin(3\psi_{r,n})/4$

of hardware impairments on BF gains in the UE's TTD array revealed how the gain, phase, and delay errors affect the beam pair misalignment probability. In numerical simulations, we showed that the proposed beam training leads to a comparable angle estimation accuracy as the EBS, while using only one OFDM symbol and low complexity DSP.

APPENDIX

The distorted gain $\bar{\alpha}_n$ is modeled as a lognormal random variable and it is straightforward to determine its moments. The terms $I_{r,n}$, and $Q_{r,n}$ are defined as $I_{r,n} = \bar{\alpha}_n\cos(\bar{\psi}_{r,n})$ and $Q_{r,n} = \bar{\alpha}_n\sin(\bar{\psi}_{r,n})$, respectively. Since $\bar{\alpha}_n$ and $\bar{\psi}_{r,n}$ are independent, it is enough to find the moments of $\cos(\bar{\psi}_{r,n})$ and $\sin(\bar{\psi}_{r,n})$ to know the moments of $I_{r,n}$, and $Q_{r,n}$.

The random variable $\bar{\psi}_{r,n}$ can be expressed as $\bar{\psi}_{r,n} = \sigma_\psi\psi_{r,n}' + \psi_{r,n}$, where $\psi_{r,n}'$ is a standard Gaussian random variable. Then the mean of the transformation $e^{j\bar{\psi}_{r,n}}$ is $E[e^{j\bar{\psi}_{r,n}}] = e^{j\psi_{r,n}}E[e^{j\sigma_\psi\psi_{r,n}'}]$. After using simple mathematical manipulations to calculate $E[e^{j\sigma_\psi\bar{\psi}_{r,n}'}]$, the mean $E[e^{j\bar{\psi}_{r,n}}]$ can be expressed as $E[e^{j\bar{\psi}_{r,n}}] = e^{-\sigma_\psi^2/2}(\cos(\psi_{r,n}) + j\sin(\psi_{r,n}))$. Using $E[e^{j\bar{\psi}_{r,n}}]$ and Euler's formula, we can conclude that $E[\cos(\bar{\psi}_{r,n})] = e^{-\sigma_\psi^2/2}\cos(\psi_{r,n})$ and $E[\sin(\bar{\psi}_{r,n})] = e^{-\sigma_\psi^2/2}\sin(\psi_{r,n})$. The results for $E[\cos(\bar{\psi}_{r,n})]$ and $E[\sin(\bar{\psi}_{r,n})]$ can be used to find higher moments of $\cos(\bar{\psi}_{r,n})$ and $\sin(\bar{\psi}_{r,n})$ and moments of their cross-terms. All used moments are summarized in Table I.

REFERENCES

[1] R. W. Heath, N. González-Prelcic, S. Rangan, W. Roh, and A. M. Sayeed, "An overview of signal processing techniques for millimeter wave MIMO systems," IEEE Journal of Selected Topics in Signal Processing, vol. 10, no. 3, pp. 436–453, Apr. 2016.

[2] K. Hosoya, N. Prasad, K. Ramachandran, N. Orihashi, S. Kishimoto, S. Rangarajan, and K. Maruhashi, "Multiple sector ID capture (MIDC): A novel beamforming technique for 60-GHz band multi-Gbps WLAN/PAN systems," IEEE Transactions on Antennas and Propagation, vol. 63, no. 1, pp. 81–96, 2015.

[3] C. Jeong, J. Park, and H. Yu, "Random access in millimeter-wave beamforming cellular networks: issues and approaches," IEEE Communications Magazine, vol. 53, no. 1, pp. 180–185, 2015.

[4] M. Bajor, T. Haque, G. Han, C. Zhang, J. Wright, and P. R. Kinget, "A flexible phased-array architecture for reception and rapid direction-of-arrival finding utilizing pseudo-random antenna weight modulation and compressive sampling," IEEE Journal of Solid-State Circuits, vol. 54, no. 5, pp. 1315–1328, 2019.

[5] M. E. Rasekh, Z. Marzi, Y. Zhu, U. Madhow, and H. Zheng, "Noncoherent mmWave path tracking," in Proceedings of the 18th International Workshop on Mobile Computing Systems and Applications, ser. HotMobile '17. New York, NY, USA: Association for Computing Machinery, 2017, p. 13–18. [Online]. Available: https://doi.org/10.1145/3032970.3032974

[6] V. Desai, L. Krzymien, P. Sartori, W. Xiao, A. Soong, and A. Alkhateeb, "Initial beamforming for mmWave communications," in 2014 48th Asilomar Conference on Signals, Systems and Computers, 2014, pp. 1926–1930.

[7] C. N. Barati, S. A. Hosseini, M. Mezzavilla, T. Korakis, S. S. Panwar, S. Rangan, and M. Zorzi, "Initial access in millimeter wave cellular systems," IEEE Transactions on Wireless Communications, vol. 15, no. 12, pp. 7926–7940, 2016.

[8] A. Alkhateeb, O. El Ayach, G. Leus, and R. W. Heath, "Channel estimation and hybrid precoding for millimeter wave cellular systems," IEEE Journal of Selected Topics in Signal Processing, vol. 8, no. 5, pp. 831–846, 2014.

[9] S. Noh, M. D. Zoltowski, and D. J. Love, "Multi-resolution codebook and adaptive beamforming sequence design for millimeter wave beam alignment," IEEE Transactions on Wireless Communications, vol. 16, no. 9, pp. 5689–5701, 2017.

[10] Y. Ghasempour, C.-Y. Yeh, R. Shrestha, D. Mittleman, and E. Knightly, "Single shot single antenna path discovery in THz networks," in Proceedings of the 26th Annual International Conference on Mobile Computing and Networking, ser. MobiCom '20. New York, NY, USA: Association for Computing Machinery, 2020. [Online]. Available: https://doi.org/10.1145/3372224.3380895

[11] V. Boljanovic, H. Yan, C. C. Lin, S. Mohapatra, D. Heo, S. Gupta, and D. Cabric, "Fast beam training with true-time-delay arrays in wideband millimeter-wave systems," IEEE Transactions on Circuits and Systems I: Regular Papers, vol. 68, no. 4, pp. 1727–1739, 2021.

[12] C.-C. Lin, C. Puglisi, E. Ghaderi, S. Mohapatra, D. Heo, S. Gupta, H. Yan, V. Boljanovic, and D. Cabric, "A 4-element 800MHz-BW 29mW true-time-delay spatial signal processor enabling fast beam-training with data communications," in ESSCIRC 2021 - IEEE 47th European Solid State Circuits Conference (ESSCIRC), 2021, pp. 287–290.

[13] H. Yan, S. Ramesh, T. Gallagher, C. Ling, and D. Cabric, "Performance, power, and area design trade-offs in millimeter-wave transmitter beamforming architectures," IEEE Circuits and Systems Magazine, vol. 19, no. 2, pp. 33–58, 2019.

[14] H. L. Van Trees, Optimum array processing: Part IV of detection, estimation, and modulation theory. Hoboken: WILEY, 2004.

[15] S. Jaeckel, L. Raschkowski, K. Börner, L. Thiele, F. Burkhardt, and E. Eberlein, "QuaDRiGa - Quasi Deterministic Radio Channel Generator, user manual and documentation," Fraunhofer Heinrich Hertz Institute, Tech. Rep. v2.2.0, 2019.